Title	Ground-space bilateral teleoperation of ETS-VII robot arm by direct bilateral coupling under 7-s time delay condition
Author(s)	Imaida, T; Yokokohji, Y; Doi, T; Oda, M; Yoshikawa, T
Citation	IEEE TRANSACTIONS ON ROBOTICS AND AUTOMATION (2004), 20(3): 499-511
Issue Date	2004-06
URL	http://hdl.handle.net/2433/50065
Right	(c)2004 IEEE. Personal use of this material is permitted. However, permission to reprint/republish this material for advertising or promotional purposes or for creating new collective works for resale or redistribution to servers or lists, or to reuse any copyrighted component of this work in other works must be obtained from the IEEE.
Type	Journal Article
Textversion	publisher; none

Ground–Space Bilateral Teleoperation of ETS-VII Robot Arm by Direct Bilateral Coupling Under 7-s Time Delay Condition

Takashi Imaida, Yasuyoshi Yokokohji, *Member, IEEE*, Toshitsugu Doi, Mitsushige Oda, and Tsuneo Yoshikawa, *Fellow, IEEE*

***Abstract*—A bilateral teleoperation experiment with Engineering Test Satellite 7 (ETS-VII) was conducted on November 22, 1999. Round-trip time for communication between the National Space Development Agency of Japan ground station and the ETS-VII was approximately seven seconds. We constructed a bilateral teleoperator that is stable, even under such a long time delay. Several experiments, such as slope-tracing task and peg-in-hole task, were carried out. Task performance was compared between the bilateral mode and the unilateral mode with force telemetry data visually displayed on a screen. All tasks were possible by bilateral control without any visual information. Experimental results showed that kinesthetic force feedback to the operator is helpful even under such a long time delay, and improves the performance of the task.**

***Index Terms*—Bilateral control, ground control, passivity, space manipulator, teleoperation, time delay.**

I. Introduction

BILATERAL CONTROL provides important force information on a remote environment to an operator. It is well known, however, that even small communication delays may destabilize the system with conventional bilateral control methods, such as symmetric position servo and force-reflecting servo [17]. Anderson and Spong [1] proposed a bilateral control law that maintains stability under communication delays by using the scattering theory. Niemeyer and Slotine [12] studied further on this problem.

It has been assumed, however, that bilateral control methods would not be effective when the time delay becomes longer than about 1 s. For example, Kim *et al.* [6], who conducted an experiment of peg-in-hole tasks using a force-reflecting servo under a time-delay condition, described it as, "*… However, this force-reflection technique can be utilized only up to an approximately 0.5- to 1-s communication time delay, since a long time delay in the force feedback loop causes the system to be unstable.*"

Manuscript received July 4, 2003. This paper was recommended for publication by Associate Editor P. Dupont and Editor I. Walker upon evaluation of the reviewers' comments.

T. Imaida was with the Department of Mechanical Engineering, Graduate School of Engineering, Kyoto University, Kyoto 606-8501 Japan. He is now with Mitsubishi Heavy Industries, Ltd., Aichi 465–0042, Japan.

Y. Yokokohji and T. Yoshikawa are with the Department of Mechanical Engineering, Graduate School of Engineering, Kyoto University, Kyoto 606-8501 Japan (e-mail: yokokoji@mech.kyoto-u.ac.jp).

T. Doi was with the National Space Development Agency of Japan, Ibaraki 305-8505, Japan. He is now with Toshiba Corporation, Tokyo 105–8001, Japan.

M. Oda is with the National Space Development Agency of Japan, Ibaraki 305-8505, Japan.

Digital Object Identifier 10.1109/TRA.2004.825271

Lawn *et al.* [9] performed one-degree-of-freedom (DOF) tasks such as pushing and positioning with time delay. They used a bilateral control law based on the scattering theory and reported, "*The passivity-based laws were not tested for delays of 1 s since their performance was very poor due to extremely low stiffness.*" Hirzinger *et al.* [2] mentioned that, "*In ROTEX, the loop delays varied from 5–7 s. Predictive computer graphics seems to be the only way to overcome this problem.*"

As Peñin *et al.* [15], [16] did, we also summarized previous works on teleoperation with force feedback under certain communication time delays in Table I [5]. All of them showed the results of real experiments. These previous works can be divided into two groups: 1) direct bilateral teleoperation without any models of the remote site and 2) model-based teleoperation with pseudo force feedback from a local model of the remote environment. From the table, it seems that when the time delay is longer than about 1 s, the model-based approach would be the only solution. However, we have been doubtful about this "1-s limitation" for the following reasons.

- Some of the observations came from the results using a conventional bilateral controller, for which stability is not guaranteed under the time-delay condition. Probably, 1 s would be the limitation to stabilize such an unstable system by human operators.
- The bilateral control based on the scattering theory guarantees the stability of the system for any time delay. However, it loses its stiffness and tends to be sticky as the time delay becomes large [13]. Again, 1–2 s would be the limitation for an operator to maneuver such a system comfortably [9]. However, the scattering theory is not the only solution to the time-delay problem, and some other types of bilateral controller can also guarantee the stability.

Instead of exactly drawing the limitation line at 1 s, our claim is, in a sense, quite natural as follows. *The time-delay limitation depends on the difficulty of the task. Even if the time delay becomes longer than 1 s, some tasks could be performed by direct bilateral teleoperation.* Actually, Ferrell [3] investigated the effect of time delays longer than 1 s in bilateral control. Although the tasks he conducted were simple positioning with force feedback, he tested several time delays up to 3 s.

In this paper, the results of a ground–space teleoperation experiment using a robot arm mounted on the Engineering Test Satellite 7 (ETS-VII) are shown. The experiment was conducted on November 22, 1999. Round-trip time for communication between the National Space Development Agency (NASDA) of

TABLE I
AMOUNT OF TIME DELAY IN PREVIOUS WORKS ON TELEOPERATION WITH FORCE FEEDBACK

Author(s)	Model-Based?	Time Delay for Round Trip	Feature
[1] Anderson & Spong (1989)	No	80ms, 400ms, 4s	Scattering Theory
[12] Niemeyer & Slotine (1991)	No	1s	Wave Variables
[6] Kim *et al.* (1992)	No	1s	Shared Compliant Control
[9] Lawn & Hannaford (1993)	No	up to 1s	Comparison between Scattering Theory and Others
[7] Kosuge *et al.* (1996)	No	1.4s	Virtual Time Delay
[14] Oboe & Fiorini (1998)	No	320ms	PD-type
[8] Kotoku (1992)	Yes	1s	Predictive Display with Force Feedback
[4] Funda *et al.* (1992)	Yes	3s	Teleprogramming
[18] Tsumaki *et al.* (1996)	Yes	5s	Velocity/Damping Control
[15] Peñin *et al.* (2000)	Yes	5-7s	Truss Structure Experiment on ETS-7

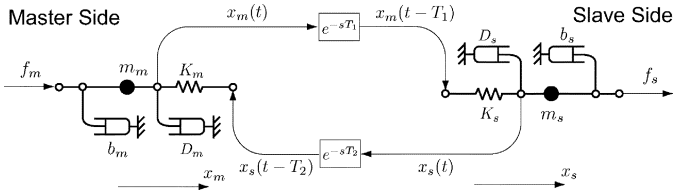

Fig. 1. PD-type bilateral control.

Japan ground station and the ETS-VII was between 6–7 s. We constructed a bilateral teleoperator using a proportional derivative (PD)-type controller that is stable even under such a long time delay. Several tasks, such as slope tracing and peg-in-hole, were carried out. All the tasks could be completed by direct bilateral control, even without using visual information. The experimental results demonstrate that kinesthetic force feedback to the operator is helpful, even under such a long time delay.

To the best of the authors' knowledge, there have not been any studies on ground–space teleoperation with *direct* force feedback yet. We would like to emphasize that what we used in the experiment was not the simulated force feedback based on a model of the remote environment, but the real force feedback from the slave side.

II. BILATERAL CONTROLLER WITH TIME DELAY

One of the well-known approaches to dealing with time delays is to use scattering transformation, as it was proposed by Anderson and Spong [1]. This approach was studied further by Niemeyer and Slotine [12], who introduced the notion of "wave variable." Besides this wave-variable approach, there are several other approaches which are less popular. For example, Leung *et al.* [10] proposed a bilateral controller for time delays based on the H_∞-optimal control and the μ-synthesis framework. Oboe and Fiorini [14] dealt with the time-varying delay problem over the Internet by using a simple PD-type controller.

We paid attention to this PD-type controller, which is shown in Fig. 1. The dynamics of master and slave arms can be formulated as follows:

$$\tau_m + f_m = m_m\ddot{x}_m + b_m\dot{x}_m \tag{1}$$

$$\tau_s - f_s = m_s\ddot{x}_s + b_s\dot{x}_s \tag{2}$$

where x_m and x_s denote respective positions of the master and slave arms, and τ_m and τ_s are the actuator driving forces. b_m and b_s represent the viscous coefficients of the driving mechanism. f_m is the force that the operator applies to the master, and f_s denotes the force that the slave arm exerts on the environment.

The PD-type controller is given by the following equations:

$$\tau_m = -K_m\left(x_m(t) - x_s(t-T_2)\right) - D_m\dot{x}_m \tag{3}$$

$$\tau_s = K_s\left(x_m(t-T_1) - x_s(t)\right) - D_s\dot{x}_s \tag{4}$$

where K_m and K_s are position gains, and D_m and D_s are damping gains. T_1 and T_2 are the time delays from the master to the slave, and from the slave to the master, respectively.

Oboe and Fiorini [14] assumed free motions of both master and slave arms, and analyzed the stability condition of this PD-type controller under time-varying delay conditions. In our experiments, however, the slave arm is not always free, and we cannot apply their stability condition. We assumed constant time delays in both directions and derived a stability condition under all passive terminations using Llewellyn's stability criteria [11]. The derived condition is given by

$$(D_m + b_m)(D_s + b_s) \geq \frac{K_m K_s (T_1 + T_2)^2}{4}. \tag{5}$$

The derivation of this condition is presented in Appendix A. As the time delays become longer, the damping gains should be increased, resulting in sticky feeling. Unlike the wave-variable-based controller, however, the apparent inertia is not affected by the time delay. Therefore, this PD-type controller is expected to still be useful, even under a long time delay in the range of 5–7 s.

From (5), one can see that we do not need the damping gains when there is no time delay. However, applying the stability condition of [14] to the case of constant time delay, one can conclude that a certain amount of damping is required even if there is no time delay. This means that the condition by Oboe and Fiorini may become more conservative than (5) for a constant time delay.

III. OVERVIEW OF THE EXPERIMENT

A. Purpose of the Experiment

In this section, the purpose of the experiment is summarized. A more detailed description of the experiment can be found in Section IV. We focus on the following three aspects:

1) check the basic performance of the PD-type bilateral controller under the condition of 5–7 s time delay;
2) check the performance of various tasks:
   a) accuracy of applied forces commanded from the ground (pushing task);
   b) accuracy of recognizing constraint surface shapes (slope-tracing task);

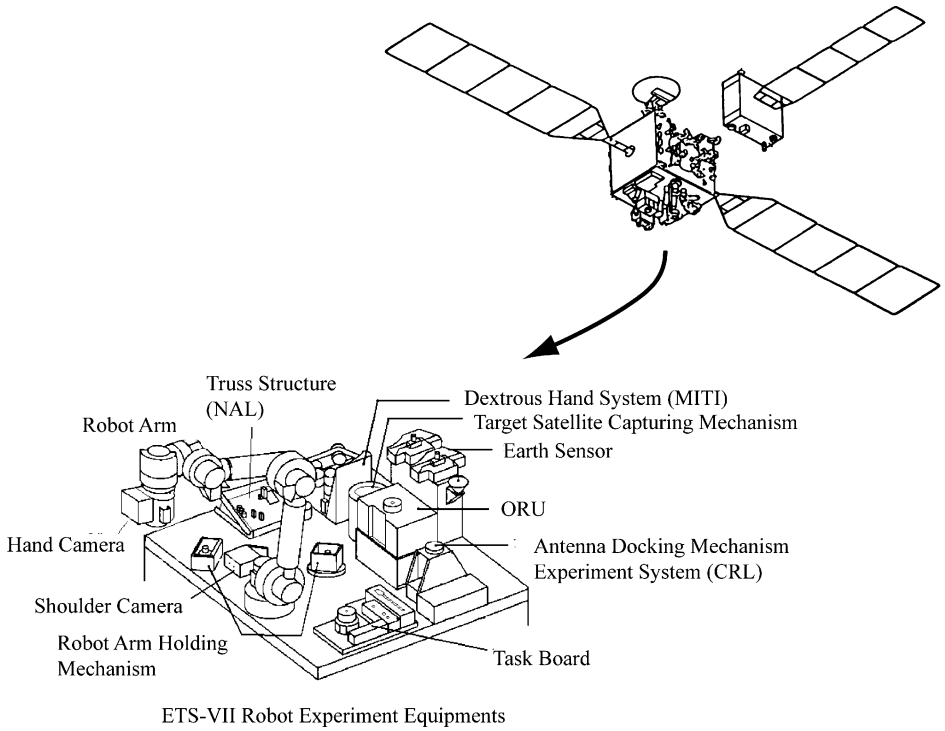

Fig. 2. Robot system on ETS-VII.

c) accuracy of recognizing contact state transitions (peg-in-hole task);
d) accuracy of recognizing unknown constraint directions (slide-handle task);

3) investigate the cognitive aspect and the skill level of the operators.

B. Experimental System

Fig. 2 shows the experimental robot system on the ETS-VII. It has a 6-DOF 2-m long robotic arm, which can be controlled remotely from the ground station. Fig. 3 illustrates the task board on the ETS-VII, which contains several experimental facilities used in the experiment. Fig. 4 shows the configuration of the experimental system. The command signal from the master handle is transmitted to the ETS-VII through the NASDA's operation equipment at a time interval of 250 ms. The controller of the master handle receives the telemetry data from the satellite, also at a time interval of 250 ms. Fig. 5(a) shows the overview of the ground control station. A 2-DOF force-feedback joystick (Impulse Engine 2000 by Immersion Co., San Jose, CA) shown in Fig. 5(b) was used as the master handle. A six-axis force/torque sensor (MICRO 5/50 by BL Autotech, Ltd., Kobe, Japan) is attached to the joystick so that the force applied by the operator can be measured. The maximum force that can be generated at the top of the master handle is approximately 3.2 N, and the stroke is approximately 15 cm in both x and y directions. The master handle is controlled by a target computer (Pentium II 450 MHz) with the VxWorks realtime operating system, and its sampling time is 1 ms.

C. Modified Bilateral Controller

The PD-type bilateral controller discussed in Section II assumes a *grounded* damper at both master and slave sides. Due to the limitation of the on-board arm controller specification of the ETS-VII, however, we could not implement such a grounded damper at the slave side. Instead, we reluctantly used a compliant controller where the damping term is *relative*, as shown in Fig. 6. Let this relative damping gain be denoted by D'_s.

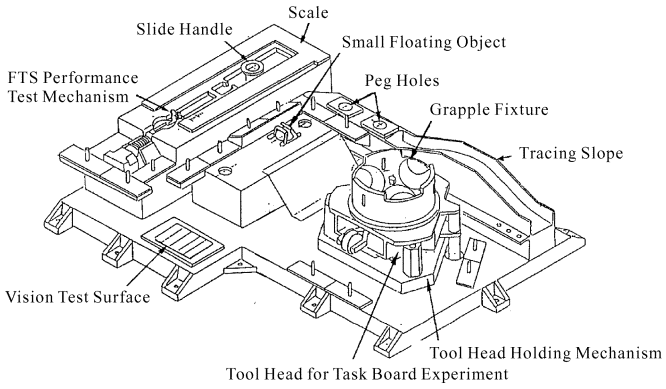

Fig. 3. Task board on ETS-VII.

We derived the stability condition for this modified controller. To guarantee the stability, the following inequality must be satisfied for all $\omega > 0$ and at $\omega \to 0$:

$$(D_m + b_m)D'_s \geq \frac{1}{2}\sqrt{\frac{K_m^2 K_s^2}{\omega^4} + \frac{K_m^2 {D'_s}^2}{\omega^2}} - \left(\frac{K_m K_s}{\omega^2}\cos\omega(T_1+T_2) + \frac{K_m D'_s}{\omega}\sin\omega(T_1+T_2)\right). \tag{6}$$

The derivation of this condition is described in Appendix B.

Unfortunately, the condition is not simple like (5), and we need to check the above inequality for all frequencies. Fig. 7 illustrates left and right sides of this inequality with appropriate

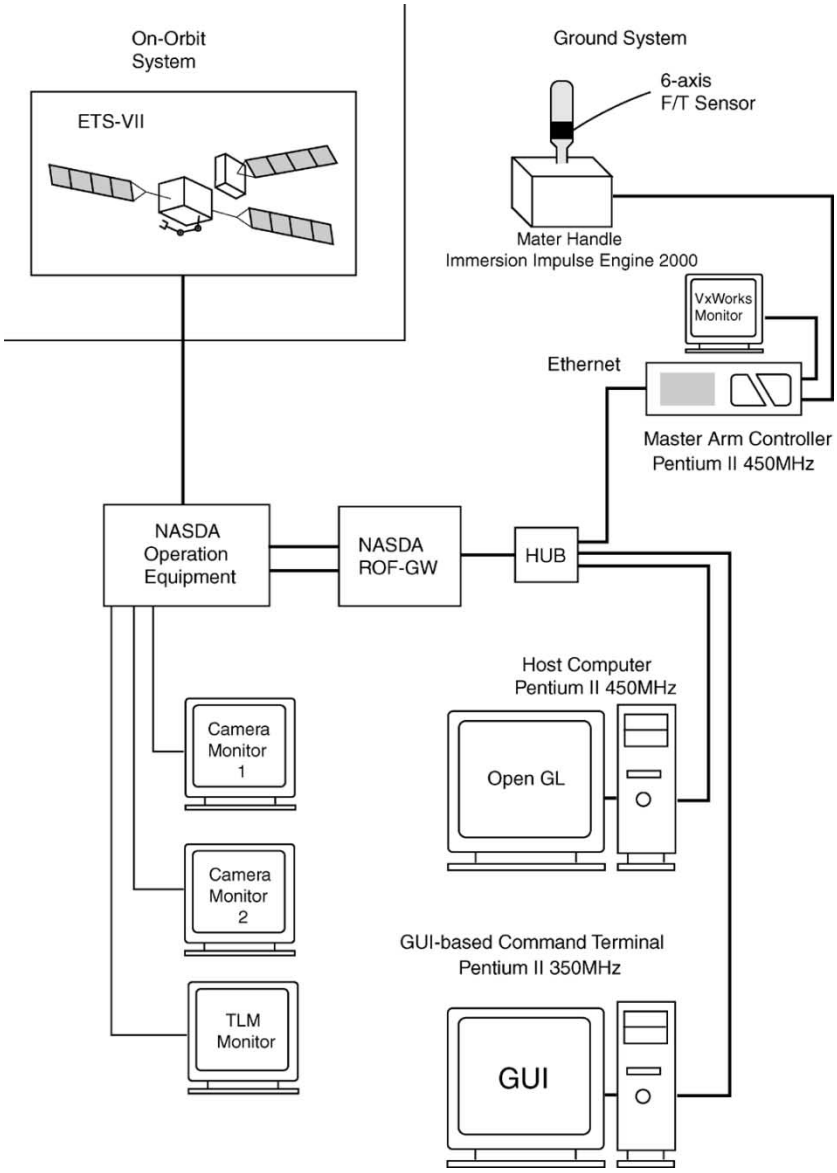

Fig. 4. Configuration of the experimental system.

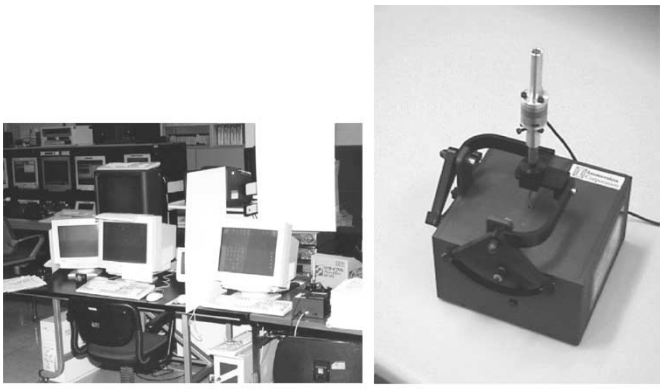

(a) control station (b) master handle

Fig. 5. Experimental system.

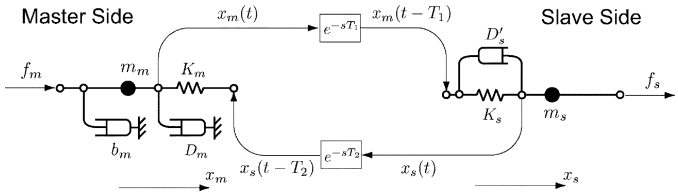

Fig. 6. Modified bilateral controller.

controller gains. One can see that checking at low frequencies, including $\omega \rightarrow 0$, is sufficient. Table II shows the gains that satisfy this condition.

Although we know that the modified controller can ensure the system stability for any passive environment and operator dynamics by applying enough damping gain, shown in Table II, we could not increase the damping gain at the master side large enough due to the hardware limitation of the master handle (mainly due to the low encoder resolution). The largest damping gain that could be achieved on our master handle was $D_m = 10$ Ns/m, which is far below the required value $D_m = 90$ Ns/m by the stability condition.

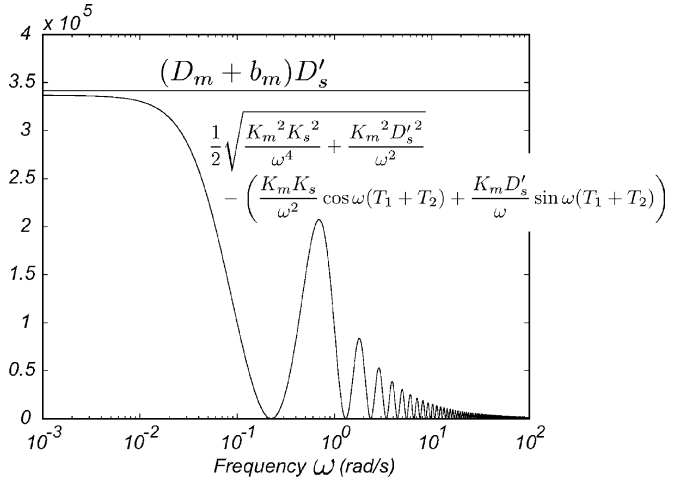

Fig. 7. Plot of stability condition.

TABLE II
GAINS THAT SATISFY THE STABILITY CONDITION

Slave velocity gain: D'_s	3795 Ns/m
Slave position gain: K_s	200 N/m
Master velocity gain: D_m	90 Ns/m
Master position gain: K_m	40 N/m

Since we know that the passivity condition is sometimes conservative, we studied whether or not we could perform the experiment with $D_m = 10$ Ns/m as follows. First, we modeled the operator and the environment by linear models (spring, mass, and damper). Next, we simulated the overall system response using representative parameters of the operator and the environment (corresponding to free motion and hard contact). Then, we confirmed that the system is stable, even with $D_m = 10$ Ns/m. Of course, this confirmation is not perfect, because we did not check all possible combinations of operator dynamics and environments. To make sure that this underdamped controller is acceptable, we checked what parameter combination makes the overall system unstable with $D_m = 10$ Ns/m. As a result, we found that the system becomes unstable only when the operator's mass is more than 1.0×10^6 kg, which is an unrealistic value. From the results of these considerations, we concluded that the system is stable, even with $D_m = 10$ Ns/m under the condition of the planned experiments and decided to perform the experiments with this underdamped controller.

In the experimental setup, the command signal and the telemetry data is transmitted at a 250-ms time interval. However, control signals for the master handle and the robot joints are updated at a higher sampling rate (about 1000 Hz). The stability analysis mentioned above was based on the framework of continuous time systems. It is one of our future works to analyze the system stability in the framework of discrete time systems with multisampling rate.

D. Specific Conditions of the Space Experiment and Preliminary Experiment on the Ground

Specific conditions of our experiment are as follows.

- Any hardware and software trouble that leads to system malfunction is not permissible. The reliability of the experimental system must be strictly assured.
- The experiment time assigned to us was limited, and it was approximately 240 min in total. The assigned time was divided into six slots called "path," corresponding to the duration time (about 40 min) when the tracking data relay satellite (TDRS) on the geostationary orbit is visible from the ETS-VII (ETS-VII itself is orbiting around the earth, 550 km above the ground). Since we need about 10 min to open and close the experiment sessions (e.g., resuming/returning the robot from/to the standby condition), a series of experiments must be completed within 30 min.
- The command signals to the robot are always monitored and checked by the NASDA operation equipment, and the maximum operating speed of the robot tip is restricted to 2.0 mm/s for safety reasons.

To check the operation of our experimental system, we performed simulation experiments over the Internet, connecting our master controller in Kyoto and the robot simulator, which was developed by NASDA, in Tsukuba before the real space experiment was carried out. The distance between Tsukuba and Kyoto is about 600 km. The NASDA simulator can simulate the motion of the robot arm mounted on the ETS-VII. However, we could simulate only the tasks on the tracing slope, and not the peg-in-hole task nor the slide-handle task, because the NASDA simulator could not handle the complex contact dynamics of these tasks. Therefore, the preliminary experiment could not cover all tasks planned in the real experiment. This was one of the limitations of the preliminary experiment on the ground. In addition, it was also difficult to simulate the real communication link exactly in the preliminary experiment, since the connection was established over the Internet.

The maximum speed of 2.0 mm/s is very slow, compared with normal operations on the ground. Theoretically speaking, there is no relationship between operating speed and stability. Practically speaking, however, the operator must move the master arm very slowly or take "move and wait" strategy under such a long time-delay condition.

IV. DETAILED CONTENTS OF THE EXPERIMENT

In this section, each experiment task will be described in detail. During the experiment, one can monitor two real images taken from the shoulder camera and the hand camera as shown in Figs. 8 and 9, respectively. As we describe in the following sections, the operators need to estimate the shape of the constraint surface, the instant of contact state transitions, and the direction of the constraint in the tasks. Since the operators must estimate those things without monitoring real scenes, we placed two masking boards in the control station so that these two real images are shielded from the operator's position, as shown in Fig. 5(a). In the following tasks, only the computer screen showing telemetry force data or nothing (depending on the experimental conditions) is visible to the operators.

A. Pushing Task

In the pushing task, the operator brings the tip of the robot arm into contact with the surface of the tracing slope (the location of the tracing slope is shown in Fig. 3). Then, he applies a rectangle force pattern $5\ \text{N} \rightarrow 15\ \text{N} \rightarrow 5\ \text{N}$ downwards without moving

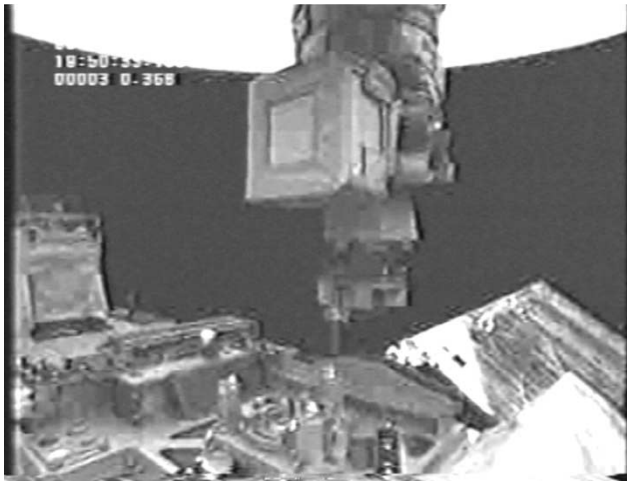

Fig. 8. Shoulder camera image (slope-tracing task).

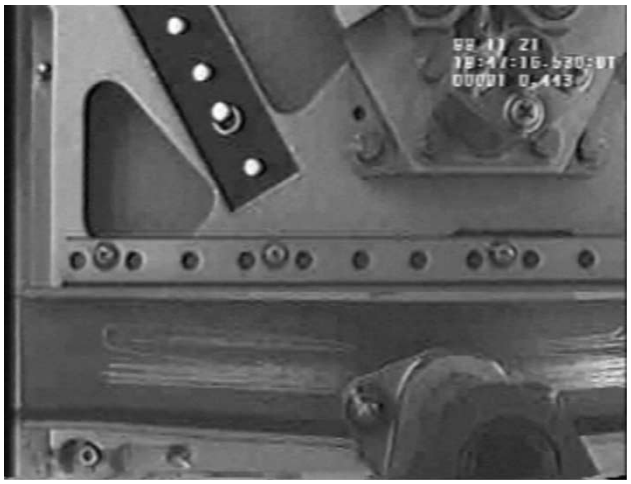

Fig. 9. Hand camera image (slope-tracing task).

the arm in tangential directions. Since the force-scaling factor between master and slave is five, the force pattern that the operator should actually apply to the master is $1\ \mathrm{N} \rightarrow 3\ \mathrm{N} \rightarrow 1\ \mathrm{N}$. Settling time and errors were evaluated in the following three cases.

Case B+T (bilateral mode + force telemetry graph): The operator can feel force feedback from the master handle. At the same time, he can monitor the telemetry force data displayed on the screen, as shown in Fig. 10.

Case B (bilateral mode): The operator must operate with force feedback alone and no visual information is provided.

Case U+T (unilateral mode + force telemetry graph): No force feedback is provided from the master handle. The telemetry force data on the screen is the only information fed back to the operator.

B. Slope-Tracing Task

In the slope-tracing task, the operator lets the robot arm contour the sinusoidal slope, while exerting a constant force (5 N). As shown in Fig. 8, a peg is attached to the tip of the robot arm. The starting point, which was not told to the operator, was chosen among points A, B, and C, shown in Fig. 11. The operator was asked to move the arm down to the surface until the tip of the arm comes into contact with the surface, then to move 150 mm left, and to move back to the starting point. Depending on the starting point, the resultant trajectory will be one of the patterns shown in Fig. 12.

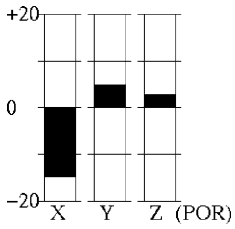

Fig. 10. Bar graph of force telemetry.

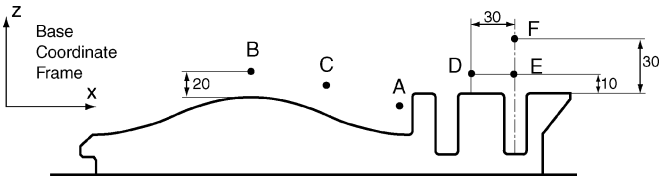

Fig. 11. Starting points for slope-tracing and peg-in-hole tasks.

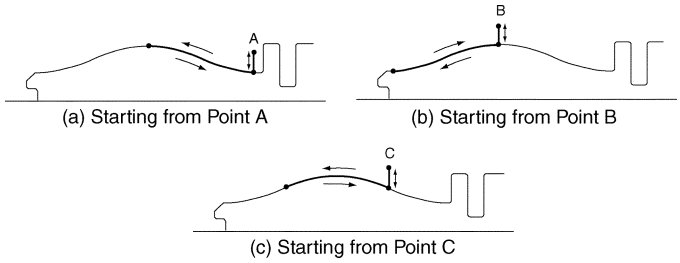

Fig. 12. Three trajectory patterns in slope-tracing task.

In order to compare the task performance under equal conditions, the operators were asked to complete this task preferably in three minutes and within the maximum of four minutes. The following two cases were tested:

Case B+T (bilateral mode + force telemetry graph);

Case U+T (unilateral mode + force telemetry graph).

Completion time and force errors were evaluated. In addition, the operator had to answer which starting point was selected after he finished each trial.

C. Peg-in-Hole Task

In the peg-in-hole task, the robot arm was initially placed at point D in Fig. 11, 30 mm left from the peg hole. The same peg used in the slope-tracing task was used again in this task. The diameter of the peg is 18 mm, and the hole has 0.4 mm clearance. For smooth insertion, the peg tip is rounded and the hole is chamfered. The operator brings the peg into contact with the top surface, slides it horizontally until it reaches the hole entrance (10 mm below point E), and then inserts the peg into the hole. The operator was asked to avoid lateral force as much as possible when inserting the peg. He was also asked to identify the transition of the contact state, i.e., the instants when the peg starts to enter the hole and when it reaches the bottom of the hole, respectively. The following three cases were tested:

Case B+T (bilateral mode + force telemetry graph);
Case B (bilateral mode);
Case U+T (unilateral mode + force telemetry graph).

Completion time, the amount of lateral force during the insertion, and accuracy of recognizing the transition of the contact state were evaluated. In fact, we were not sure if this peg-in-hole task was possible under such a long time delay.

For the above three tasks (pushing, tracing, and peg-in-hole), two-dimensional (2-D) horizontal motions of the master handle were assigned to 2-D translational motions of the robot arm in the vertical plane across the contouring slope and peg holes. The orientation of the arm and the remaining translational component were fixed by the on-board position controller.

D. Slide-Handle Task

In the slide-handle task, the slide handle in the slide guide, which can be seen in Fig. 3, was used. 2-D horizontal motions of the master handle were assigned to 2-D translational motions in the horizontal plane, including the sliding direction. To make the sliding direction unknown to the operator, a certain amount of rotational coordinate transformation around the normal axis of the horizontal plane was introduced.

At the initial stage, the peg attached to the tip of the robot arm was already inserted in the hole of the slide handle, and this handle was placed at the center of the slider guide. The operator should estimate the unknown sliding direction by probing the master handle. Then, he should move the robot to one end of the slider guide, then to the other end, and finally move back to the center. The operator was asked to minimize lateral forces (perpendicular to the sliding direction) as much as possible when moving the slide handle.

The operator should complete the task within three minutes. To complete the task, he must estimate the correct sliding direction and recognize the end of the slider guide as fast as possible. After the task, the operator should report his estimation of the sliding direction. The following three cases were tested:

Case B+T (bilateral mode + force telemetry graph);
Case B (bilateral mode);
Case U+T (unilateral mode + force telemetry graph).

Completion time, the amount of lateral force during the sliding motion, and accuracy of the estimated sliding direction were evaluated. Here, we were also uncertain whether or not this task was possible under such a long time-delay condition before the experiment.

E. Skill Level and Other Cognitive Factors

Due to the limited time assigned to us, most of the experiments were carried out by a single operator, who was accustomed to the system operation using the master handle. To investigate the effect of skill level, two other operators conducted some tasks. One was a NASDA operator, who had been accustomed to the operation of the ETS-VII robot arm by NASDA's teleoperation facilities, but was not familiar with the master handle used in this experiment. The other one was a novice operator, who had not been trained with any device, but had a background of teleoperation.

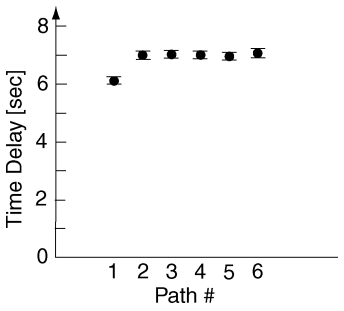

Fig. 13. Measured time delay for round trip.

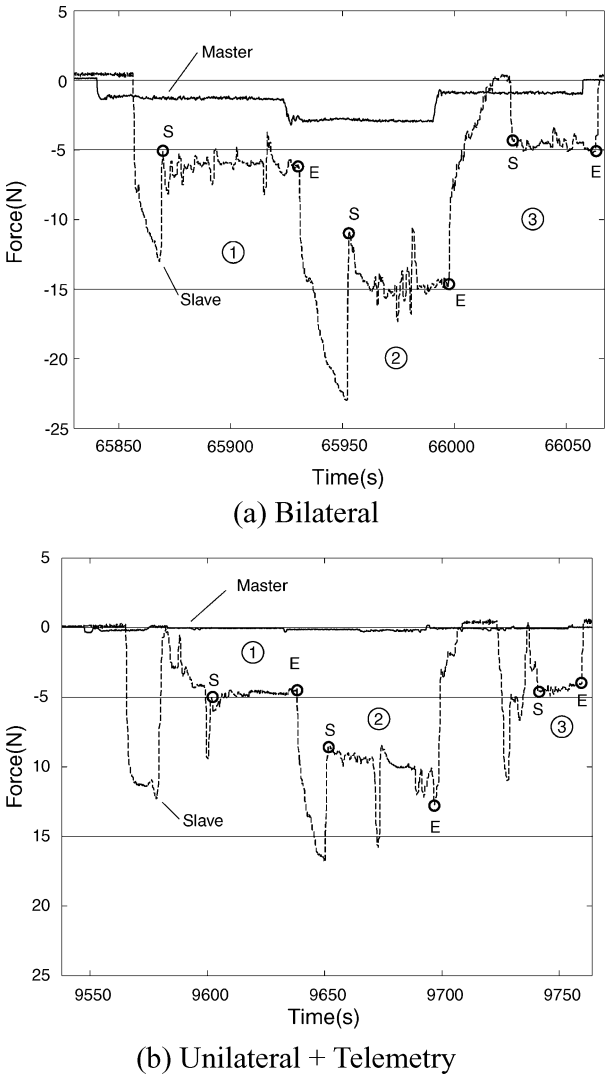

Fig. 14. Force responses in pushing task.

To investigate cognitive factors, such as mental load and their attention points during the tasks, the operators were asked to fill out a questionnaire after the experiment.

V. Experimental Results

The experiment was conducted on November 22, 1999. Round-trip time for communication between the control station at the NASDA Tsukuba Space Center and the ETS-VII, flying

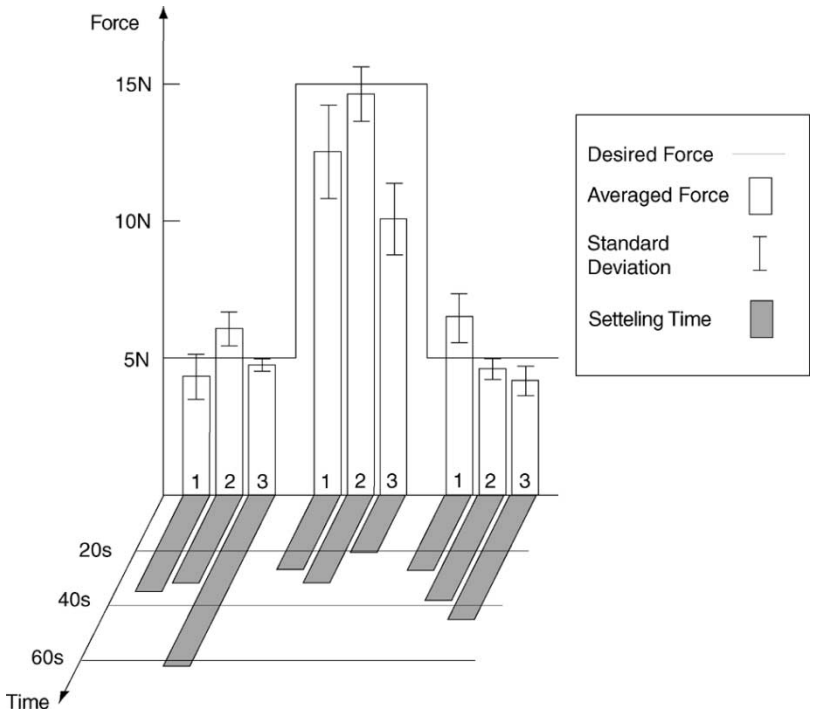

Fig. 15. Result of pushing task (Task 1: B+T, Task 2: B, Task 3: U+T).

TABLE III
ACTUAL STARTING POINTS AND DECLARED POINTS BY THE OPERATORS

Task Condition	Staring Point	Declared Point	Judgement
Task 1 (Bilateral + Telemetry)	A	C	×
Task 2 (Bilateral + Telemetry)	C	C	○
Task 3 (Unilateral + Telemetry)	C	C	○
Task 4 (NASDA Operator) (Bilateral + Telemetry)	C	C	○
Task 5 (longer operation time) (Bilateral + Telemetry)	B	B	○

at an orbit 550 km above the ground, was approximately 6–7 s. Fig. 13 shows the measured time delay at each "path." One can see that time delay differs between each path, but does not fluctuate so much within each path. Figs. 8 and 9 are snapshots taken during the slope-tracing task experiment.

A. Pushing Task

Fig. 14 shows two typical examples of the force response during the pushing tasks with the bilateral mode and unilateral-plus-telemetry mode, respectively. One can see that the bilateral mode reaches the desired force more quickly and accurately than the unilateral mode. Fig. 15 summarizes the results of the pushing task.

B. Slope-Tracing Task

Table III shows the results of the estimation of the starting points by the operators. Except for Task 1, the operators, including the NASDA operator, could estimate the starting points correctly. We cannot clearly explain why the operator failed in Task 1. One possibility would be due to some psychological factors, such as stress for the first trial or not being accustomed to the experiment. It should be noted, however, that in the bilateral mode, the shape estimation became confident from the beginning with only a little movement of the handle, whereas in the unilateral mode, the estimation was quite uncertain, even after the entire movement. Fig. 16 can help to understand the reason for this observation. This figure shows typical arm trajectories (top) and force responses (bottom) in the bilateral mode and unilateral-plus-telemetry mode, respectively. In the bilateral mode, the trajectory of the master handle reproduces the slope shape, while in the unilateral mode, it is difficult to estimate the slope shape from the master handle trajectory. From the force response, one can see that in the unilateral mode, sometimes the robot arm loses contact with the tracing slope. It means that tracing the slope was difficult in the unilateral mode.

Fig. 17 summarizes the experimental results of the tracing task. The stroke in the task with the unilateral mode had to be reduced to 130 mm, 20-mm shorter than the initial plan, to go back to the starting point within the time limit. Like the pushing task, with the bilateral mode, one could adjust the applied forces to the desired value more accurately and complete the task faster than with the unilateral mode. It is interesting to notice that the performance of Task 1 (i.e., the task when the operator failed to estimate the correct starting point) was not bad. Of course, the correct answers of the starting points were disclosed only after all trials were executed.

We should also note that the task performance of the NASDA operator, who used this system for the first time, was comparable to that of the skilled operator.

C. Peg-in-Hole Task

Fig. 18 shows the arm trajectories of the peg-in-hole task. In the figure, the actual position of the peg, which corresponds to

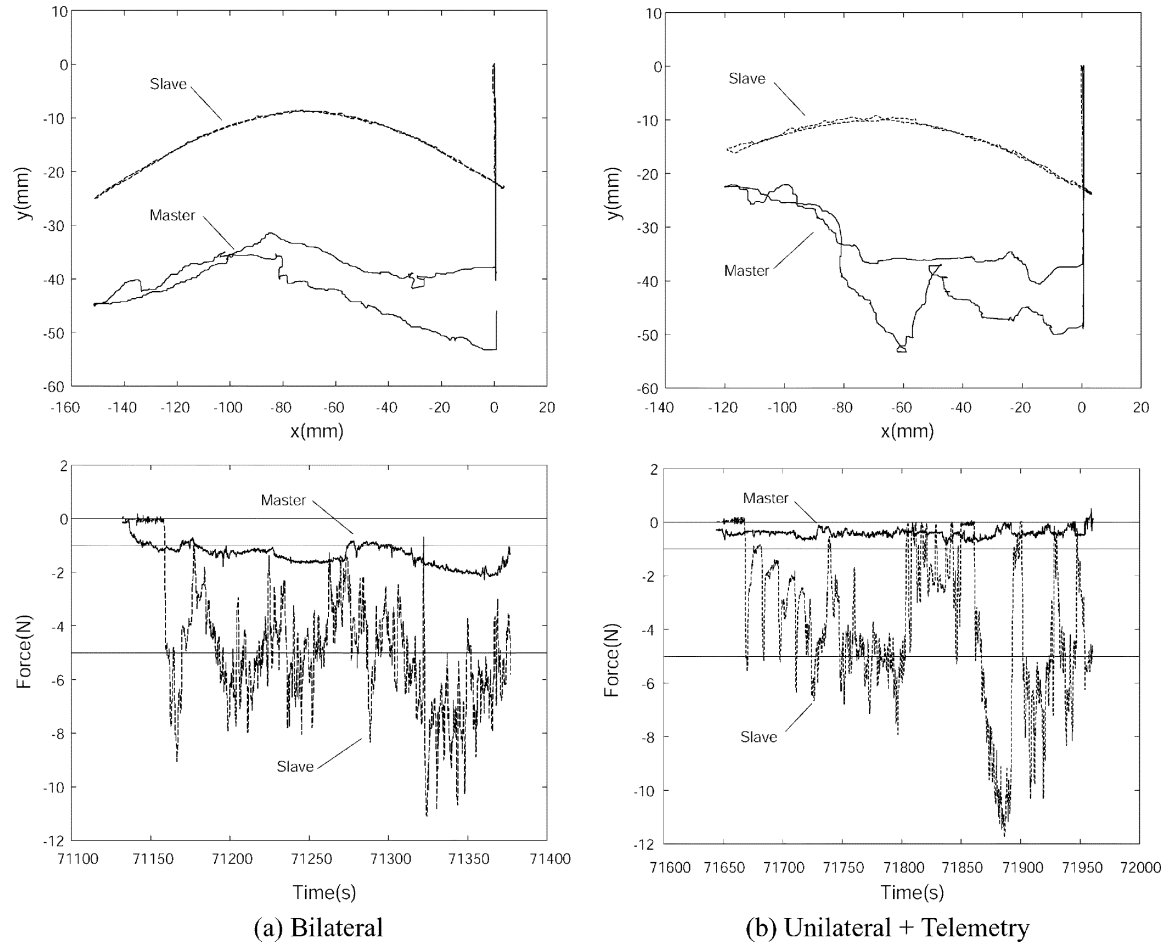

Fig. 16. Typical arm trajectories and force responses in slope-tracing task.

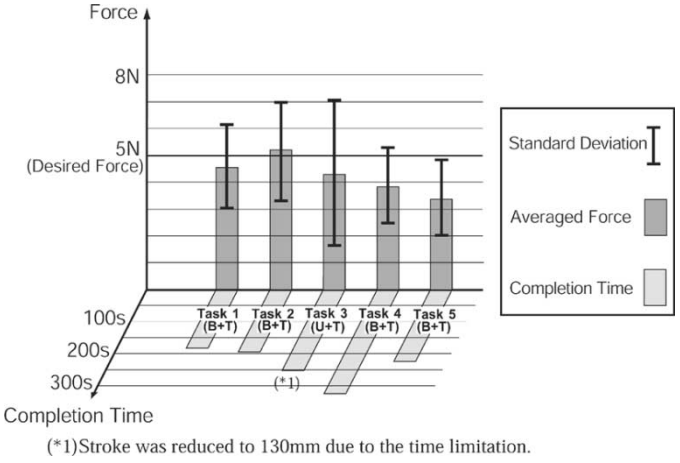

Fig. 17. Result of slope-racing task (task numbers correspond to those in Table III).

the timing when the operator judged the starting point of the insertion, is also drawn. One can see that in the bilateral mode, the operator could identify the transition of contact state accurately only using the force-feedback information. On the other hand, the recognition of a new contact when the peg reached the bottom of the hole was better when using only telemetry data, rather than using force feedback from the master handle. The times when the operator declared the bottom-reaching were 18, 15, and 5 s after the peg had actually reached the bottom in Task 1, Task 2, and Task 3, respectively. Fig. 19 summarizes the results of the peg-in-hole task. In contrast to what we expected, the unilateral mode gave smaller lateral forces than the bilateral mode did. Our explanation of this observation is that the operator moved the master arm carefully in the unilateral mode, while he moved the master arm relying on the reaction force from the hole in the bilateral mode. The trajectory of the master handle in Fig. 18 supports this explanation. One can see that the position deviation of the master from the centerline of the hole is smaller in the unilateral mode than in the bilateral mode.

D. Slide-Handle Task

Table IV shows the results of the estimation of the sliding direction in the slide-handle task. In all cases, the operators could estimate the sliding direction with reasonable accuracy. It should be noted, however, that in the bilateral mode, the operator was already confident at a very early stage of the task. Only a little movement of the handle was sufficient for them to identify the sliding direction. In the unilateral mode, they were quite uncertain about their estimation, even after the entire movement. This observation is similar to the previous observation drawn from the slope-tracing task. Fig. 20 shows a typical example of the hand trajectory of the slide-handle task with the bilateral mode. In the figure, the inserted rotational transformation was

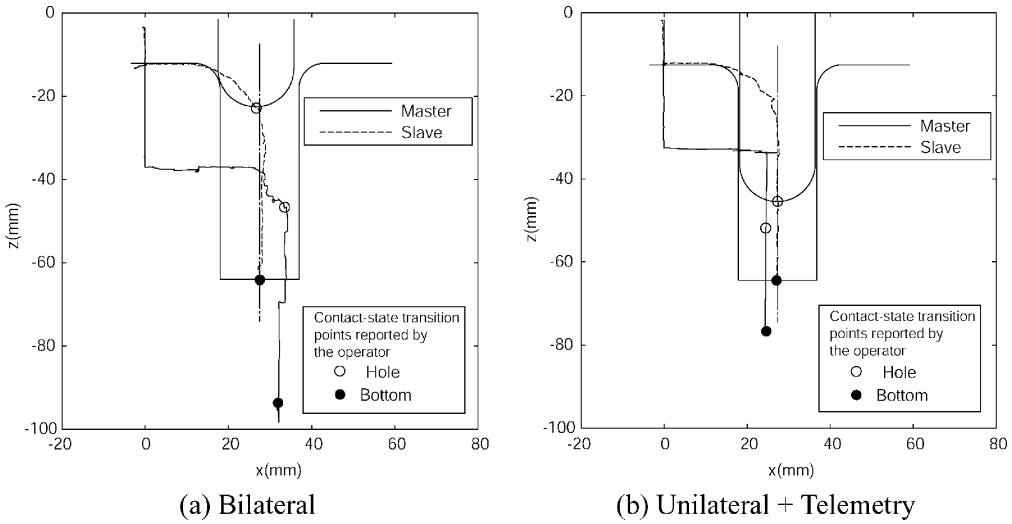

Fig. 18. Arm trajectories during the peg-in-hole task.

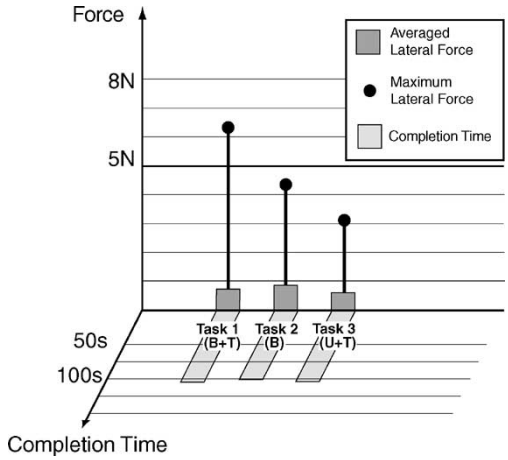

Fig. 19. Result of peg-in-hole task (Task 1: B+T, Task 2: B, Task 3: U+T).

TABLE IV
SLIDING DIRECTIONS AND DECLARED DIRECTIONS

Task	Rotation angle[deg]	Declared angle[deg]
Task 1 (Bilateral + Telemetry)	-75	-65
Task 2 (Bilateral)	0	0
Task 3 (Unilateral + Telemetry)	20	30
Task 4 (NASDA Operator) (Bilateral + Telemetry)	60	45
Task 5 (Novice Operator) (Bilateral + Telemetry)	-60	-45

canceled, so ideally the master and slave trajectories should coincide. One can see that the operator moved the handle in the wrong direction at the beginning, but shifted to the correct direction later, feeling the force feedback from the handle.

All operators, including the NASDA operator and the novice operator, could complete the task in the bilateral mode. In the unilateral mode, however, the operator should stop moving the handle only halfway and could not complete the task within the assigned time. The NASDA operator performed only the probing task to estimate the sliding direction.

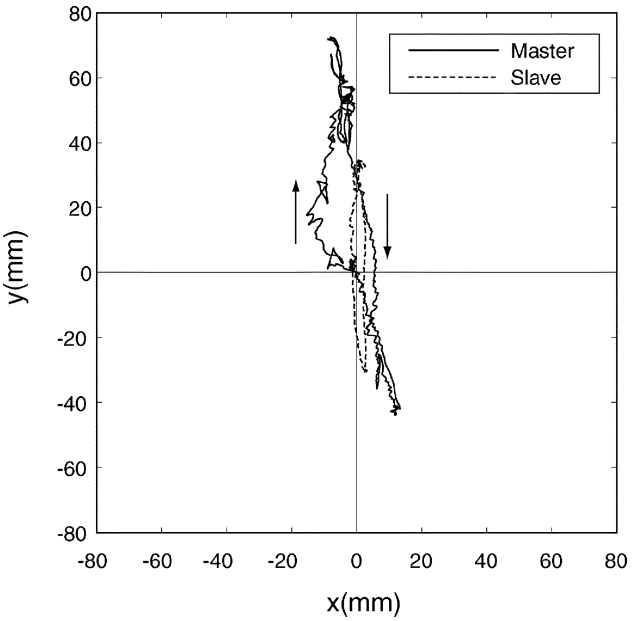

Fig. 20. Typical arm trajectory in slide handle task (Task 1: Bilateral mode, rotated -75°).

Fig. 21 summarizes the results of the slide-handle task. In contrast to what we expected, the amount of lateral forces could not be reduced in the bilateral mode. This is because the operator exerted large lateral forces when probing the sliding direction at the beginning of the task. This observation is similar to the previous observation in the peg-in-hole task. After the direction was estimated, the lateral forces became small.

E. Discussion

From the questionnaire survey after each task, the following observations were obtained.

- All three operators paid most of their attention to the force feedback from the master handle, even when the telemetry force data was displayed on the screen.

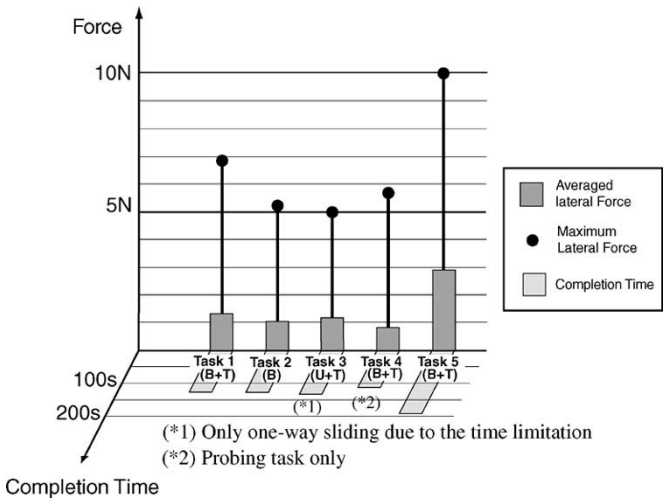

Fig. 21. Result of slide-handle task (task numbers correspond to those in Table IV).

- Using the kinesthetic force-feedback information, the operators could recognize the shape of the contouring slope as well as the entrance of the peg hole with just a small movement. As for the instant of the contact with the environment (e.g., when the peg reached the bottom of the hole), however, it was difficult to recognize for the operator only from the kinesthetic force feedback, due to the low position gain of the bilateral controller.
- The telemetry force data was noisy and difficult to use for shape recognition. The data should have been passed through a lowpass filter.
- Even a novice operator could complete the task, showing that no specific skill level is required to use this teleoperation system.

It was surprising, even for us, that the kinesthetic force-feedback information was useful and could improve the task performance, even under such a long time delay. Of course, the task should be performed slowly, and the maneuverability is lower than the case without time delay. However, this experiment does prove that it is possible to complete some tasks by direct bilateral control, even under 6–7 s time-delay conditions.

VI. Conclusion

In this paper, the results of a ground–space teleoperation experiment using a robot arm mounted on the ETS-VII were shown. Stability conditions for a PD-type bilateral controller were derived. Due to the limitation of the onboard robot controller of the ETS-VII, the controller was modified, and also a modified stability condition was derived. Several tasks, such as a slope-tracing task and a peg-in-hole task, were carried out under 6–7 s time-delay conditions. All the tasks were possible by using the direct bilateral control, even without using any visual information. The experimental results demonstrate that force feedback to the operator is still helpful, even under such a long time delay. To the best of the authors' knowledge, this experiment is the first ground–space teleoperation by *direct* bilateral control. Since the number of experiments was limited, and also, only a few subjects joined the experiments, we need further experiments to confirm the obtained results.

In this paper, we have only shown the possibility of performing some tasks under 6–7 s time delays. Please note, however, that we are not claiming that bilateral control under 6–7 s conditions is practically useful. It is needless to say that a shorter time delay gives better maneuverability. Although the ETS-VII is orbiting just 550 km above the earth, the amount of delayed time (6–7 s) is considerably large. Since most of the time delay is due to the data transmission in the computer network on the ground, it is technically possible to make the delay time 1–2 s or less, even if the data is relayed through a satellite on the geostationary orbit.

So far, we have been trying to manage a *given* time delay on *existing* data communication infrastructures. These infrastructures were designed without considering the use of direct bilateral teleoperation from the ground. However, if we could expect a breakthrough to improve the maneuverability of teleoperation with a time delay shorter than 6–7 s, we could take a completely new approach, i.e., we would first define the time-delay limitation for given tasks, and then construct a communication link to achieve this time delay. This point is what we really want to emphasize in this paper. To proceed with this approach, we need to investigate the relationship between the task complexity and the allowable time delay in more detail. For this purpose, laboratory experiments, where delay time can be changed easily, would be appropriate. As a benchmark test, the LEGO block assembly, which was proposed by the authors [20], might be useful to evaluate the task complexity.

Appendix A
Derivation of Stability Condition (5)

The impedance matrix describing the teleoperator shown in Fig. 1 is given by

$$\boldsymbol{Z}_{mss} = \begin{bmatrix} m_m s + b_m + D_m + \frac{K_m}{s} & \frac{K_m e^{-sT_2}}{s} \\ \frac{K_s e^{-sT_1}}{s} & m_s s + b_s + D_s + \frac{K_s}{s} \end{bmatrix}. \tag{7}$$

Applying Llewellyn's stability criterion [11] to (7), we can find that the teleoperator is stable if the following three conditions are satisfied at all frequencies:

$$B_m \geq 0 \tag{8}$$

$$B_s \geq 0 \tag{9}$$

$$\begin{aligned} 4\Big(B_m B_s + \frac{K_m K_s}{\omega^2}\cos\omega T_1 \cos\omega T_2\Big) & \\ \times \left(B_m B_s - \frac{K_m K_s}{\omega^2}\sin\omega T_1 \sin\omega T_2\right) & \\ - \left(\frac{K_m K_s}{\omega^2}\sin\omega T_2 \cos\omega T_1 \right. & \\ \left. - \frac{K_m K_s}{\omega^2}\sin\omega T_1 \cos\omega T_2\right)^2 \geq 0 & \end{aligned} \tag{10}$$

where we set $B_m = b_m + D_m$ and $B_s = b_s + D_s$. Note that equal relations are allowed in the above inequalities because the stability bound is also acceptable in the framework of teleoperation. Equation (10) assumes $\omega \neq 0$, and we cannot check the stability at $\omega = 0$. Instead, we check for $\omega \to 0$.

Solving (10) for B_mB_s, we get

$$B_mB_s \geq \frac{K_mK_s}{2\omega^2}(-\cos\omega(T_1+T_2)+1) \tag{11}$$

or

$$B_mB_s \leq \frac{K_mK_s}{2\omega^2}(-\cos\omega(T_1+T_2)-1). \tag{12}$$

Assuming that (8) and (9) are satisfied, we can disregard (12).

Rewriting the right-hand side of (11), we get the following inequality:

$$\begin{aligned}\frac{K_mK_s}{2\omega^2}(1-\cos\omega(T_1+T_2)) &= K_mK_s\frac{\sin^2\frac{\omega(T_1+T_2)}{2}}{\omega^2}\\ &\leq K_mK_s\frac{(T_1+T_2)^2}{4}.\end{aligned} \tag{13}$$

The equal relation in the inequality is achieved at a limit for $\omega \to 0$.

From (11) and (13), we get the stability condition given by

$$B_mB_s \geq \frac{K_mK_s(T_1+T_2)^2}{4}. \tag{14}$$

Appendix B
Derivation of Stability Condition (6)

With the modified bilateral controller, the impedance matrix becomes

$$\boldsymbol{Z}_{mss} = \begin{bmatrix} m_ms+b_m+D_m+\frac{K_m}{s} & \frac{K_me^{-sT_2}}{s} \\ \frac{K_se^{-sT_1}}{s}+D'_se^{-sT_1} & m_ss+D'_s+\frac{K_s}{s}\end{bmatrix}. \tag{15}$$

Applying Llewellyn's stability criterion [11] to (15), the following three conditions must be satisfied at all frequencies:

$$B_m \geq 0 \tag{16}$$

$$D'_s \geq 0 \tag{17}$$

and

$$\begin{aligned}&4\left(B_mD'_s+\frac{K_m}{\omega}\cos\omega T_2\left(\frac{K_s}{\omega}\cos\omega T_1+D'_s\sin\omega T_1\right)\right)\\ &\times\left(B_mD'_s+\frac{K_m}{\omega}\sin\omega T_2\left(D'_s\cos\omega T_1-\frac{K_s}{\omega}\sin\omega T_1\right)\right)\\ &-\left(\frac{K_m}{\omega}\sin\omega T_2\left(\frac{K_s}{\omega}\cos\omega T_1+D'_s\sin\omega T_1\right)\right.\\ &\left.+\left(D'_s\cos\omega T_1-\frac{K_s}{\omega}\sin\omega T_1\right)\frac{K_m}{\omega}\cos\omega T_2\right)^2 \geq 0\end{aligned} \tag{18}$$

where we again set $B_m = b_m + D_m$.

Modifying (18), we get

$$\begin{aligned}&4B_m^2{D'_s}^2+4B_mD'_s\left(\frac{K_mK_s}{\omega^2}\cos\omega(T_1+T_2)\right.\\ &\left.+\frac{K_mD'_s}{\omega}\sin\omega(T_1+T_2)\right)-\left(\frac{K_mK_s}{\omega^2}\sin\omega(T_1+T_2)\right.\\ &\left.-\frac{K_mD'_s}{\omega}\cos\omega(T_1+T_2)\right)^2 \geq 0.\end{aligned} \tag{19}$$

Solving (19) for B_mB_s, we get

$$\begin{aligned}B_mD'_s \geq \frac{1}{2}&\left(\sqrt{\frac{K_m^2K_s^2}{\omega^4}+\frac{K_m^2{D'_s}^2}{\omega^2}}-\left(\frac{K_mK_s}{\omega^2}\cos\omega(T_1+T_2)\right.\right.\\ &\left.\left.+\frac{K_mD'_s}{\omega}\sin\omega(T_1+T_2)\right)\right)\end{aligned} \tag{20}$$

or

$$\begin{aligned}B_mD'_s \leq -\frac{1}{2}&\left(\sqrt{\frac{K_m^2K_s^2}{\omega^4}+\frac{K_m^2{D'_s}^2}{\omega^2}}+\left(\frac{K_mK_s}{\omega^2}\cos\omega(T_1+T_2)\right.\right.\\ &\left.\left.+\frac{K_mD'_s}{\omega}\sin\omega(T_1+T_2)\right)\right).\end{aligned} \tag{21}$$

From (16) and (17), we need $B_mD'_s \geq 0$. Therefore, only (20) needs to be satisfied. This condition inequality corresponds to (6).

We can analytically derive that the left-hand side (LHS) of (20) goes to $(K_mK_s/4)\left((D'_s/K_s)-(T_1+T_2)\right)^2$ as $\omega \to 0$. Unlike the previous case in Appendix A, the value of the LHS of (20) may exceed this limit. Therefore, we have to check (20) until we reach sufficiently small ω, and check whether $B_mD'_s \geq (K_mK_s/4)\left((D'_s/K_s)-(T_1+T_2)\right)^2$ is satisfied.

Acknowledgment

The authors would like to thank R. Kikuue and H. Iida, graduate students of Kyoto University, Kyoto, Japan, who joined the experiment as the satellite operation procedure commander and the telemetry observer, respectively. They would also like to express their appreciation to Dr. W.-K. Yoon and other members of the Uchiyama Laboratory of Tohoku University, Sendai, Japan, for their helpful comments about the experiment. Finally, they express their gratitude to N. Inaba (NASDA), Dr. Y. Fukusima (NASDA), N. Shouji (Space Engineering Development Co., Ltd.), Y. Uchibori (NASDA), H. Kawauchi (Toshiba Co.), S. Nishida (Toshiba Co.), K. Tanabe (NASDA), and other people who joined the experiment.

References

[1] R. J. Anderson and M. W. Spong, "Bilateral control of teleoperators with time delay," *IEEE Trans. Automat. Contr.*, vol. 34, pp. 494–501, May 1989.

[2] G. Hirzinger *et al.*, "Sensor-based space robotics—ROTEX and its telerobotic features," *IEEE Trans. Robot. Automat.*, vol. 9, pp. 649–663, Oct. 1993.

[3] W. R. Ferrell, "Delayed force feedback," *Human Factors*, pp. 449–455, 1966.

[4] J. Funda *et al.*, "Teleprogramming: Toward delay-invariant remote manipulation," *PRESENCE, Teleoperators, Virtual Environ.*, vol. 1, no. 1, pp. 29–44, 1992.

[5] T. Imaida *et al.*, "Ground–space bilateral teleoperation experiment using ETS-VII robot arm with direct kinesthetic coupling," in *Proc. IEEE Int. Conf. Robotics and Automation*, 2001, pp. 1031–1038.

[6] W. S. Kim *et al.*, "Force reflection and shared compliant control in operating telemanipulators with time delay," *IEEE Trans. Robot. Automat.*, vol. 8, pp. 176–185, Apr. 1992.

[7] K. Kosuge *et al.*, "Bilateral feedback control of telemanipulators via computer network," in *Proc. IEEE/RSJ Int. Conf. Intelligent Robots and Systems*, 1996, pp. 1380–1385.

[8] T. Kotoku, "A predictive display with force feedback and its application to remote manipulation system with transmission time delay," in *Proc. IEEE/RSJ Int. Conf. Intelligent Robots and Systems*, 1992, pp. 239–246.

[9] C. A. Lawn and B. Hannaford, "Performance testing of passive communication and control in teleoperation with time delay," in *Proc. IEEE Int. Conf. Robotics and Automation*, vol. 3, 1993, pp. 776–783.
[10] G. M. H. Leung *et al.*, "Bilateral controller for teleoperators with time delay via μ-synthesis," *IEEE Trans. Robot. Automat.*, vol. 11, pp. 105–116, Feb. 1995.
[11] F. B. Llewellyn, "Some fundamental properties of transmission systems," *Proc. IRE*, vol. 40, no. 5, pp. 271–283, 1952.
[12] G. Niemeyer and J. J. E. Slotine, "Stable adaptive teleoperation," *IEEE J. Ocean. Eng.*, vol. 16, pp. 152–162, Jan. 1991.
[13] ——, "Designing force-reflecting teleoperators with large time delays to appear as virtual tools," in *Proc. IEEE Int. Conf. Robotics and Automation*, 1997, pp. 2212–2218.
[14] R. Oboe and P. Fiorini, "A design and control environment for internet-based telerobotics," *Int. J. Robot. Res.*, vol. 17, no. 4, pp. 433–449, 1998.
[15] L. F. Peñin, K. Matsumoto, and S. Wakabayashi, "Force reflection for time-delayed teleoperation of space robots," in *Proc. IEEE Int. Conf. Robotics and Automation*, 2000, pp. 3120–3125.
[16] L. F. Peñin and K. Matsumoto, "Teleoperation with Time Delay—A Survey and its Use in Space Robotics," Nat. Aerosp. Lab., Tokyo, Japan, Rep. TR-1438T, 2002.
[17] T. B. Sheridan, "Space teleoperation through time delay: Review and prognosis," *IEEE Trans. Robot. Automat.*, vol. 9, pp. 592–606, Oct. 1993.
[18] Y. Tsumaki *et al.*, "Virtual-reality-based teleoperation which tolerates geometrical modeling errors," in *Proc. IEEE/RSJ Int. Conf. Intelligent Robots and Systems*, 1996, pp. 1023–1030.
[19] ——, "Verification of an advanced space teleoperation system using internet," in *Proc. IEEE/RSJ Int. Conf. Intelligent Robots and Systems*, 2000, pp. 1167–1172.
[20] Y. Yokokohji, Y. Iida, and T. Yoshikawa, "Toy problem as the benchmark test for teleoperation systems," *Adv. Robot.*, vol. 17, no. 3, pp. 253–273, 2003.

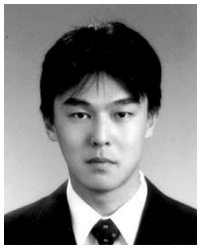

Takashi Imaida was born in Kyoto, Japan, on October 4, 1975. He received the B.S. degree in engineering science in 1998, and the M.S. degree in mechanical engineering in 2000, both from Kyoto University, Kyoto, Japan.

He is currently with Nagoya Aerospace Systems, Mitsubishi Heavy Industries, Ltd., Aichi, Japan, where he works in flight-control system design.

Mr. Imaida is a member of the Robotics Society of Japan.

Yasuyoshi Yokokohji (M'91) was born in Osaka, Japan, on August 4, 1961. He received the B.S. and M.S. degrees in precision engineering in 1984 and 1986, respectively, and the Ph.D. degree in mechanical engineering in 1991, all from Kyoto University, Kyoto, Japan.

From 1988 to 1989, he was a Research Associate in the Automation Research Laboratory, Kyoto University. From 1989 to 1992, he was a Research Associate in the Division of Applied Systems Science, Faculty of Engineering, Kyoto University. From 1994 to 1996, he was a Visiting Research Scholar at the Robotics Institute, Carnegie Mellon University, Pittsburgh, PA. He is currently an Associate Professor in the Department of Mechanical Engineering, Graduate School of Engineering, Kyoto University. His current research interests are robotics and virtual reality, including teleoperation systems, vision-based tracking, and haptic interfaces.

Dr. Yokokohji is a member of the Institute of Systems, Control and Information Engineers (Japan), the Robotics Society of Japan, the Society of Instruments and Control Engineers (Japan), the Japan Society of Mechanical Engineers, the Society of Biomechanisms of Japan, the Virtual Reality Society of Japan, and ACM.

Toshitsugu Doi received the B.S. degree in mechanical engineering, and the M.S. degree in applied systems science, from Kyoto University, Kyoto, Japan, in 1990 and 1992, respectively.

He is now with Toshiba Co., Tokyo, Japan, as a Specialist in the Space Robotics Division. During 1998–2000, he was with the National Space Development Agency of Japan, Ibaraki, Japan, where he was a member of the ETS-VII project team.

Mr. Doi is a member of the Robot Society of Japan.

Mitsushige Oda received the M.S. degree in control engineering in 1977, and the Dr. Eng. degree in 1996, both from the Tokyo Institute of Technology (Tokyo Tech.), Tokyo, Japan.

Since 1977, he has been working for the National Space Development Agency of Japan (NASDA), Ibaraki, Japan, being engaged in R&D of satellite attitude-control systems, conceptual designs of new space systems, and development of space robot systems. He is currently a Senior Researcher with NASDA and also a Visiting Professor with Tokyo Tech. (Note: NASDA was reorganized as the Japan Aerospace Exploration Agency (JAXA) on October 1, 2003.)

Tsuneo Yoshikawa (M'73–SM'98–F'00) received the Ph.D. degree in applied mathematics and physics from Kyoto University, Kyoto, Japan, in 1969.

Since 1969, he has been with Kyoto University, where he is currently Professor of Mechanical Engineering. From 1973 to 1975, he was an NRC Resident Research Associate at NASA Marshall Space Flight Center, Huntsville, AL. He is the author of *Foundations of Robotics* (Cambridge, MA: MIT Press, 1990). His current research interests include robotics, haptic virtual reality, and control of nonlinear mechanical systems.

Dr. Yoshikawa has received several awards, including the 1995 JDSMC Best Paper Award from the Dynamic Systems and Control Division of the ASME, and the 1997 ICRA Best Conference Paper Award from the IEEE Robotics and Automation Society.